J. Fluid Mech. (1979), *vol.* 91, *part* 1, *pp.* 131–154
Printed in Great Britain

An experimental determination of transition limits in a vertical natural convection flow adjacent to a surface

By R. L. MAHAJAN† AND B. GEBHART
Department of Mechanical Engineering, State University of New York at Buffalo

(Received 21 September 1977 and in revised form 4 February 1978)

This paper reports the results of an experimental investigation to determine transition mechanisms and limits in gases at high pressure levels. We sought also to refine further the parameters for transition, in particular the role of kinematic viscosity. In flow adjacent to a vertical uniform-flux surface in nitrogen, pressures to 16 atm were used. Both mean and disturbance quantities for the temperature and velocity fields were measured for various values of the heat flux, downstream location and ambient pressure level. Hot-wire and fine thermocouple probes were used. We found that the velocity and thermal fields remain closely coupled. Velocity, or fluid-dynamic, transition is immediately followed by thermal transition. Each was detected as a decrease in the rate of increase of both the maximum velocity and the overall temperature difference, respectively, from the laminar downstream trends. Also, the ends of transition for the velocity and the thermal fields, respectively, signalled by no further appreciable change in the intermittency distributions, were simultaneous. These results re-affirm the finding that the events of transition are not correlated by the Grashof number alone. An additional dependence on both downstream location and pressure level arises. A fixed value of the parameter $Q_{BT} = qB^{\frac{1}{15}} = 290$ characterizes the beginning of transition, where q is the fifth root of the local non-dimensional wall heat flux and B is the unit Grashof number. The end of transition, on the other hand, is best correlated by $Q_{ET} = QB^{\frac{1}{30}} = 11{\cdot}4$, where Q is the fifth root of the local non-dimensional total heat convected in the boundary region. A re-examination of other transition studies, in both gases and liquids, supports these correlations, although many such data were not determined with fast response to local sensors. There remains a small level of uncertainty in establishing exact limits for transition, since the apparently proper standards for determining them are very difficult to apply precisely in experiments. However, such limits are very important in separating regimes of different transport mechanisms.

1. Introduction

The large effort spent in research on stability and disturbance growth amply attests the great importance, and perhaps even the primacy, of the general need to establish bounds between laminar and turbulent transport regimes. The most important matter is to establish predictive parameters for the transition from laminar to turbulent flow. However, there have been few successes in this among the many flow

† Present address: Western Electric Company, Inc., Engineering Research Center, P.O. Box 900, Princeton, New Jersey 08540.

0022-1120/79/4070-5930 $02.00

configurations of great practical importance. For example, there is still some uncertainty as to what kind of disturbances lead to transition in both Pouseuille and forced boundary-layer flows, after many decades of work on each.

In buoyancy-induced flow, however, the agreement between extensive analytical and experimental investigations in recent years has added significantly to the understanding of the sequence of events leading to and during transition. Two-dimensional disturbances dominate the early stages of instability. These simple oscillations are suggested by both schlieren and interferometric observations; see, for example, Eckert & Soehngen (1951). Local sensors also indicate a nearly perfectly sinusoidal disturbance form. The initial behaviour and amplification characteristics of these disturbances in several flow configurations are now well explained in terms of linear stability theory.

For flow adjacent to a flat vertical surface, let x be the distance along the surface measured from the leading edge. Stability calculations by Dring & Gebhart (1968) have shown that, as a disturbance is convected downstream, i.e. in the direction of increasing x, disturbance components amplify selectively and in a very narrow band of frequencies. There is very strong experimental corroboration of these predictions. For a recent review of these and related matters, see Gebhart (1973) and Gebhart & Mahajan (1975).

Further downstream, nonlinear and three-dimensional effects become important, as evidenced by the earlier experimental studies by Eckert, Hartnett & Irvine (1960) and Colak-Antic (1964) in air and by Szewczyk (1962) in water. Audunson & Gebhart (1976) included spanwise effects in their analysis of disturbance growth in air and found that nonlinear interactions of two- and three-dimensional disturbances generate a mean secondary double longitudinal vortex system. This flow modification then promotes favourable conditions for even more rapid disturbance growth, in forming a region of high shear. An alternative spanwise steepening and flattening of the base velocity is predicted. These results agree with the experimental findings of Colak-Antic and have since been substantiated in detail by experimental measurements by Jaluria & Gebhart (1973). The longitudinal vortex system has been directly associated with the beginning of transition; see the measurements of Jaluria & Gebhart (1973, 1974).

After the three-dimensional disturbance growth, transition begins. Except for the recent studies by Godaux & Gebhart (1974) and Jaluria & Gebhart (1974), which will be discussed later, there are relatively few measurements of fundamental flow quantities at either the beginning of or during transition. Regnier & Kaplan (1963) studied the transition and turbulent regimes adjacent to an isothermal vertical plate in air and in pressurized carbon dioxide. From interferometer visualization they inferred that the local condition for transition to turbulence could not be expressed by the local Grashof number alone. However, they do not report any systematic dependence of a transition Grashof number on any other physical quantities. Some inferences concerning transition may be drawn from the turbulent natural convection flow studies by Warner (1966), Warner & Arpaci (1968) and Cheesewright (1968) in air and by Lock & Trotter (1968) and Vliet & Liu (1969) in water. However, these studies relate quantitatively to transition in suggesting empirical values or range of the Grashof number which approximately mark the beginning and end of transition.

The expected success of Grashof number criteria was suggested both by tradition and by linear stability analysis. For example, we now know that the growth rate of

Reference	Fluid	Pr‡	G_{BT}	G^*_{BT}	x (cm)	P (atm)	Instrument used to detect transition	Q_{BT} or Q_{ET}	Symbol (figures 10 and 11)	$\frac{Q_{BT}}{Q_{BT}\dagger}$ or $\frac{Q_{ET}}{Q^\dagger_{ET}}$
					Beginning of transition					
Present study	N_2	0·71	—	388–620	13·2–33	1–15·92	Hot wire	290†	See figure 10	1
	N_2	0·71	—	400–650	13·2–33	1–15·92	Thermocouple	305†	See figure 10	1
Warner & Arpaci (1968)	Air	0·72	466	—	65	1	Thermocouple	290	◐	0·95
Colak-Antic (1964)	Air	0·72	572	—	84	1	Hot wire	318	△	1·1
Cheesewright (1968)	Air	0·72	≃600	—	≃72	1	Thermocouple	350	▽	1·15
Regnier & Kaplan (1963)	Air	0·72	622	—	92	1	Interferometer	341	●	1·12
	CO_2	0·77	460–547	—	12·5	4–9		367–373	▽	1·20–1·22
	CO_2	0·77	645–702	—	25	4–9		355–385	▼	1·16–1·26
	CO_2	0·77	541	—	17	5		343	○	1·12
	CO_2	0·77	605	—	25	5		283	▼	0·93
	CO_2	0·77	378	—	9	10		280	○	0·92
Eckert & Soehngen (1951)	Air	0·72	400	—	61	1	Interferometer	263	■	0·86
Hugot *et al.* (1971)	Air	0·70	724	—	80·4	1	Interferometer	410	□	1·34
			665		64	1		411	□	1·35
					End of transition					
Present study	N_2	0·71	—	495–980	13·2–33	4·18–15·92	Hot wire and Thermocouple	11·4†	See figure 11	1
Cheesewright (1969)	Air	0·72	845	—	115	1	Thermocouple	11·89	▼	1·04
Hugot *et al.* (1971)	Air	0·70	936	—	113·4	1	Interferometer	13·26	■	1·16
			851		89	1		14·05	■	1·23

† Best-fit values from our data. ‡ Prandtl number of ambient medium.

TABLE 1. Transition data in gases.

Reference		Pr‡	G^*_{BT} —	G_{BT}	x (cm)	Instrument used to detect transition	Q_{BT} or Q_{ET}	ΔT (°C)	$\frac{\mu_\infty}{\mu_0}$
				Beginning of transition					
Jaluria & Gebhart (1974)		6·7	504–802		38·1–121·9	Hot wire thermocouple	341†	≃4·4	1·12
			563–802		38·1–121·9		381†		
Godaux & Gebhart (1974)		6·7	528–979		36·2–100	Thermocouple	379–464	3–6	1·12–1·18
Vliet & Liu (1969)	V_4	6·2	855		79	Thermocouple	435	2.2	1·063
	V_3	6·4	955		61		529	7·7	1·2
	V_2	6·4	900		35·3		588	24·1	1·62
	V_5	5·05	960		28		645	36·2	1·80
Lock & Trotter (1968)		11·0	293		24	Thermocouple hot wire	402	17·8	1·58
		11·4	368		27·4		481	35·6	2·42
Szewczyk (1962)		6·7		534	40	Flow viscualization using dye	398	6·44	1·18
				End of transition					
Jaluria & Gebhart (1974)		6·7	870		61	Hot wire and thermocouple	10·94	≃2	≃1·07
			990		83·8		10·62		
			1140		100·7		10·84		
			1320		121·9		11·75		
Vliet & Liu (1969)	V_4	6·2	1140		113	Thermocouple	10·18	0·85	1·03
	V_3	6·4	1195		80·7		12·67	5	1·12
	V_2	6·4	1385		60·5		16·96	14·8	1·38
	V_5	5·05	1615		53·6		18·73	21·9	1·50

† Best-fit value. ‡ Prandtl number of ambient medium.

TABLE 2. Transition data in water.

two-dimensional disturbances depends solely on the local Grashof number. This led Hieber & Gebhart (1971) to identify, from past data, a broad range of Grashof numbers for the beginning of transition due to naturally occurring disturbances. This was in terms of the amplification-ratio values obtained from linear stability calculations. Past actual measured transition conditions in gases and in water (see tables 1 and 2) show the wide range of Grashof number data.

This situation led Godaux & Gebhart (1974) to experiments with a tall surface, in water. The beginning of thermal transition was judged by traverses with a $2{\cdot}54 \times 10^{-3}$ cm diameter thermocouple probe at various downstream locations x, at difference surface heat flux levels q'' for each location. These data suggested that thermal transition from naturally occurring disturbances began at an approximately constant value of $(Gr_x^*)^{\frac{1}{5}}/x^{\frac{3}{5}} \propto (q''x)^{\frac{1}{5}} = [Q'(x)]^{\frac{1}{5}}$. That is, transition began when the local thermal energy Q' convected in the boundary region, at a downstream location x had reached a particular value. Here $Gr_x^* = g\beta_t q'' x^4/k\nu^2$, where q'' is the uniform time-average surface heat flux, k is the thermal conductivity, ν is the kinematic viscosity, β_t is the coefficient of thermal expansion and g is the acceleration due to gravity. For isothermal conditions, the Grashof number Gr_x is defined as $g\beta_t x^3 \Delta T/\nu^2$, where ΔT is the unchanging temperature difference across the boundary region.

This surprising result generated a much more detailed investigation by Jaluria & Gebhart (1974), also in water. Using both hot-wire and thermocouple probes, velocity transition was found to precede thermal transition. Each was found to begin at a different particular value of $G^*/x^{\frac{2}{5}}$, where $G^* = 5(\frac{1}{5}Gr_x^*)^{\frac{1}{5}}$. The two values were chosen as those at which the sensor records first showed additional higher frequency components. These components were superimposed on the selectively amplified laminar frequency, which was always almost exactly that predicted by linear stability theory for the local flow condition.

This new quantity is proportional to the fifth root of the local kinetic energy flux. It was generalized as $E = G^*(\nu^2/gx^3)^{\frac{2}{15}}$. The indicated values of E were 13·6 and 15·2 for the beginning of velocity and thermal transition, respectively. Values of E were also calculated from the transition data of other investigators. For different fluids, over the Prandtl number range 0·7–11·85 and for both isothermal and uniform-flux surface conditions, the spread in E was about 60 %; see table 1 of Jaluria & Gebhart (1974).

The end of transition was much more approximately correlated by $G^*/x^{0.54}$. This limit was defined as the downstream location beyond which the turbulent intermittency distributions across the boundary region, of both the velocity and the temperature disturbances, were found simultaneously to achieve an asymptotic form. No general dimensionless predictive parameter was proposed for this condition.

Although these last two studies very much improved the predictability of transition, the specific detailed measurements were made only in water. There was no information of comparable accuracy for transition for gases. Not even mean velocity measurements during transition were available. Nothing was known of the mechanisms.

For air ($Pr \simeq 0{\cdot}7$), the velocity and thermal boundary layers are of approximately the same thickness. In water, the thermal layer is contained well within the velocity boundary layer. This was expected to have a significant effect on the transition mechanism. Also, the predictive parameter E is still somewhat arbitrary in that the factor $(\nu^2/g)^{\frac{2}{15}}$ was introduced only for non-dimensionalization, not on specific physical

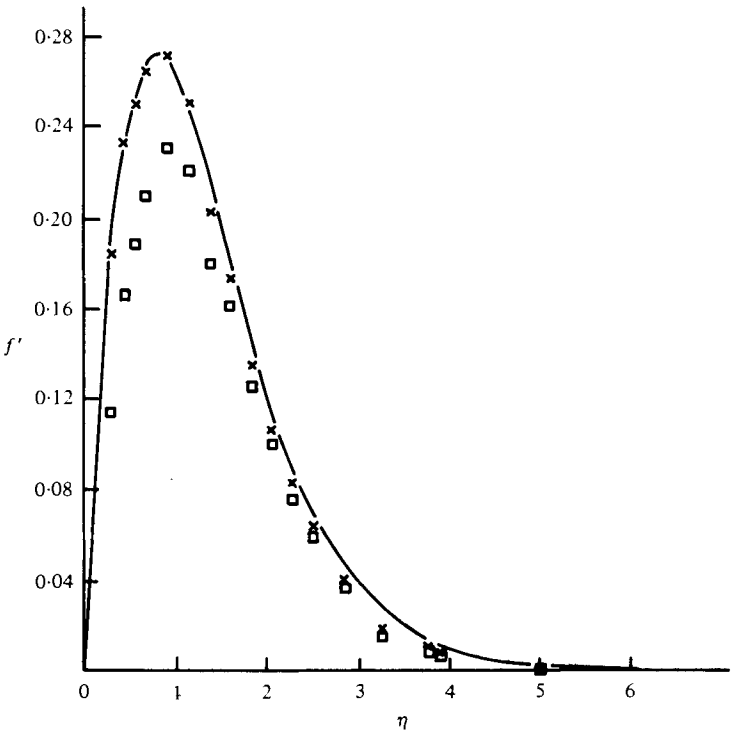

FIGURE 1. Mean velocity profiles across the laminar boundary layer for $Pr = 0{\cdot}733$ at $G^* = 230$. —, theoretical tangential velocity distribution. Data: □, uncorrected hot-wire velocity data; ×, data corrected for varying local ambient temperature.

grounds. This, for example, imposes a particular dependence of G^* on ν at the beginning of transition. Since ν is sharply density dependent in gases, this may be tested in experiments at various pressure levels.

Our investigation was undertaken to determine transition mechanisms in gases at a level of detail comparable to the information now available for water. A uniform-flux vertical surface generated flow in pressurized nitrogen. Detailed mean velocity and temperature distributions, along with disturbance data, were determined for various values of x, q'' and P, where P is the pressure in atmospheres. The disturbance frequency, intermittency distributions and turbulence-structure data are also reported. On the basis of present and previous data, more general predictive parameters for both the beginning and the end of transition in gases, as well as in liquids, are proposed.

2. The experiment

The electrically heated surface was a $2{\cdot}54 \times 10^{-3}$ cm thick Inconel-600 foil, 15·25 cm wide and 38·5 cm high. The foil was stretched between two accurately ground knife-edges so that it was flat. The foil assembly was placed in a large insulated steel test chamber with a height of 76 cm and inside diameter of 35 cm. Pre-purified, oil-free, dry bottled nitrogen was used for pressurization.

The hot-wire anemometer was a DISA 55D01. The miniature probe (DISA 55P14) was L-shaped so that the wire was upstream of the probe support. This minimized

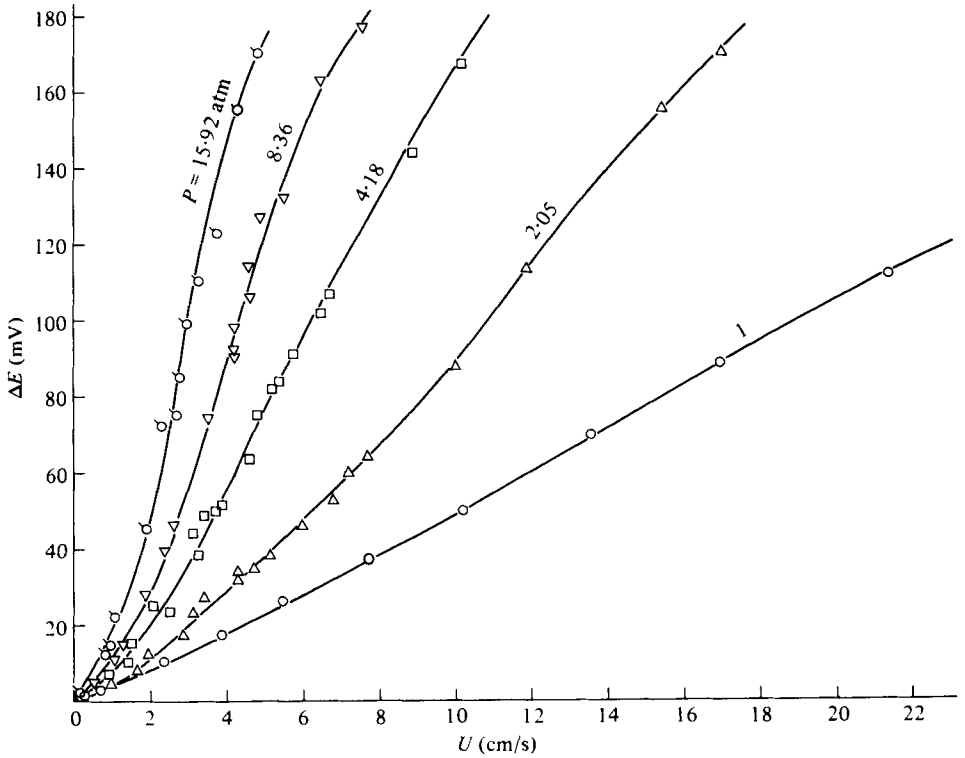

FIGURE 2. Hot-wire calibration curves for wire overheat ratio of 1·6 at different pressures, where $\Delta E = V_B - V_{B0}$, where V_B is the bridge voltage and the subscript 0 refers to the no-flow condition.

probe-support interference. The sensor was 5 μm platinum-plated tungsten wire with length–diameter ratio $L/D \simeq 250$. An overheat ratio of 1·6 was used in the final measurements. Wire response was first determined in the natural, mixed and forced flow modes, with different values of the overheat-ratio and levels of pressure. These results are discussed in detail by Mahajan & Gebhart (1977).

A different kind of calibration technique was necessary to achieve high pressure levels. It was performed in a laminar natural convection boundary layer, where the velocity was calculated. The basis for this was a conventional calibration at 1 atm. The laminar profile was then measured at 1 atm (square data points in figure 1). Upon correcting the anemometer results for varying local ambient temperature across the boundary layer, we obtained excellent agreement with the velocity calculated from theory. The difference is around 1 % in the vicinity of the maximum velocity; see figure 1. On the basis of this agreement, hot-wire calibrations at higher pressures were determined in the laminar velocity profile generated adjacent to the foil surface, with the velocities calculated from theory. The resulting calibration curves at various pressures are reproduced in figure 2.

The boundary-layer temperature measurements were made using a $5{\cdot}08 \times 10^{-3}$ cm copper–constantan thermocouple. The two thermocouple leads were horizontal and parallel to the foil for about 0·5 cm on each side of the junction. Thus the wires lay essentially along an isotherm, reducing thereby the conduction loss through the leads. These leads were then passed through a pair of 0·8 mm hollow glass tubes which were

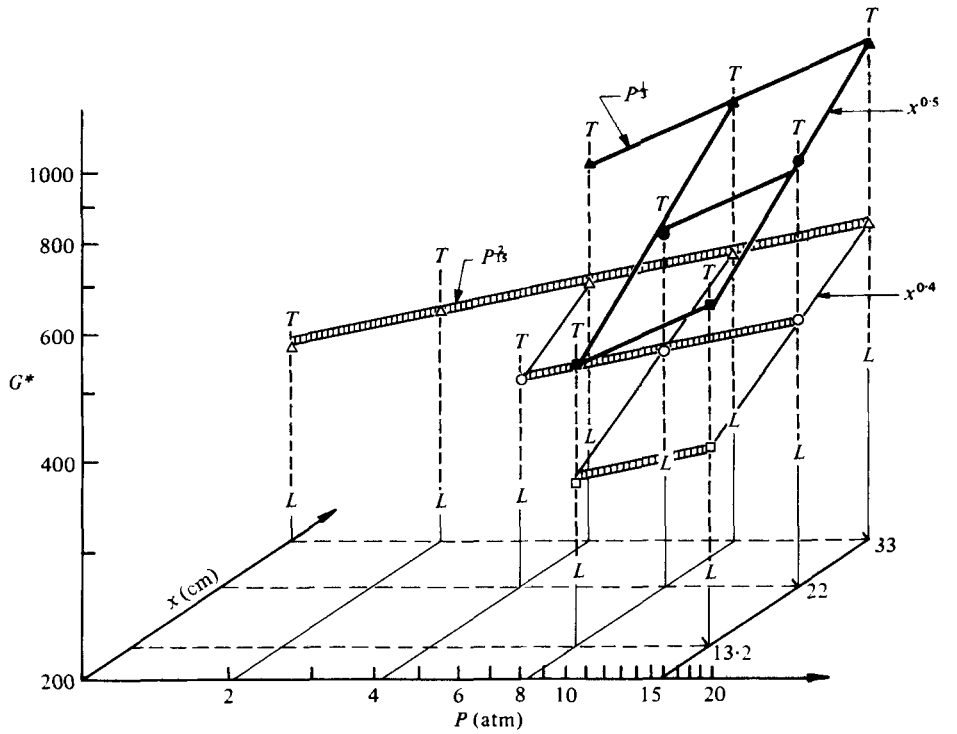

FIGURE 3. Ranges of various parameters covered in the experiment and boundaries of transition. L, T, lower and upper value of G^* investigated respectively; III, beginning of transition; ——, end of transition.

in turn attached to a support outside the boundary region. This support, which also held the hot-wire prove and a surface probe, could be moved to any location normal to the foil in the boundary layer by a DISA 55H01 remote-controlled traversing mechanism. The surface probe was a 1·5 mm diameter stainless-steel rod and was used to locate the surface through an electrical circuit. For details of these and other experimental aspects, see Mahajan (1977).

Detailed measurements were made at different downstream locations x at various levels of P and q''. All were chosen to result in local flow conditions in various stages of transition. Figure 3 shows, schematically, the range of parameters used in the experiment, as well as eventual findings concerning limits of transition. The lower and upper values in the range of G^* investigated at each x for different pressures are marked by L and T, respectively. The conditions of transition are those we determined in terms of G^*, there being an additional dependence on both x and P. The hatched area represents the beginning of transition, the bounding lower and upper lines corresponding to the limits of velocity and thermal transition, respectively. The end of transition, on the other hand, is shown by thick lines.

3. Experimental results and observations

3.1. *Beginning of transition*

Our first exploratory measurements inducated that the criterion of Jaluria & Gebhart (1974) for the beginning of transition, i.e. the presence of a higher frequency superimposed on a single laminar filtered frequency, could not be used unambigously in a gas over our whole range of x, P and q''. In purely laminar flow, we found a single filtered laminar disturbance frequency only for values of G^* greater than about 400. For lower values, there were generally two superimposed disturbance frequencies, yet the flow was still laminar.

This is predicted by the detailed stability calculation of Hieber & Gebhart (1971), for a Prandtl number of 0·07. The stability plane has been replotted in figure 8 as $B^* = 2\pi f(g\beta_t q''/k)^{\frac{1}{2}}$ *vs.* G^*, where f is the physical frequency. We have calculated additional amplitude contours for $A = 0{\cdot}5$, 1, 4 and 6. Recall that A is the downstream integral, from the neutral curve, of α_i, the downstream spatial amplification rate. Constant-B^* lines on this plane are lines of constant physical frequency downstream for any given flow condition (P, q'').

These A contours indicate no sharp frequency filtering at low G^* for this particular Prandtl number. The preference for essentially a single disturbance frequency arises only further downstream. Under certain conditions, for high flux levels, we found that transition begins in this low G^* range.

Two other, more conventional criteria for the beginning of transition are modification of local heat-transfer characteristics or the presence of significant aperiodic fluctuations. However, these are insensitive and imprecise measures. We found instead that $U_{\max}$, the observed local maximum value of the base flow velocity across the boundary region, was a much sharper indicator. The beginning of its downstream deviation from the calculated laminar trend of increase was taken here as the indication of the beginning of velocity transition.

Velocity transition occurred first. It was almost immediately followed by thermal transition, which was taken to begin at the downstream location where the value of ΔT, the temperature difference across the boundary layer, had started to decrease from the calculated laminar trend of increase downstream. Thermal transition was found to begin at a value of G^* about 4 % higher. Local values of G^* at the beginning and end of transition will be designated as G^*_{BT} and G^*_{ET}, respectively.

Our experimentally determined values of G^*_{BT} for different levels of pressure at different downstream locations are plotted in figure 3. For a fixed level of pressure, our values of G^*_{BT} show a systematic variation with the location x at which transition occurs at different levels of q''. At each pressure level, we found that the x, q'' interdependence is

$$G^*_{BT} \propto x^{\frac{2}{5}}. \tag{1}$$

Jaluria & Gebhart (1974) report the same value of the exponent of x from their measurements in water. Next, at a given downstream location, the values of G^*_{BT} at which transition began indicated the following dependence on pressure at different levels of q'':

$$G^*_{BT} \propto P^{\frac{2}{15}} \propto \rho^{\frac{2}{15}} \propto \nu^{-\frac{2}{15}}. \tag{2}$$

The same trend is found at three downstream locations; see also figure 10. The value of ν used in evaluating G^*_{BT} is calculated at the actual pressure level.

x (cm)	P (atm)	q'' (W/m²)	G†	B†	Symbol
22	8·36	9·73	350	1, 1·3	⊙
		28·50	434	1·25	×
		42·51	470	1·32	○
		59·68	503	1·37	◒
		87·50	543	1·25	◐
		120·61	579	1·25	◓
		157·83	611	—	●
		211·77	648	—	⊗
33	4·18	52·55	514	1·27	△
		65·42	537	1·21	▲
		96·15	580	1·30	◭
		134·21	620	1·255	◬
		183·46	660	1·27	▲
		303·69	730	—	◬
33	8·36	11·74	560	1·31	▽
		13·99	580	1·25	▼
		24·73	650	1·26	▽
		69·83	800	1·45	▼
		106·22	870	—	⩛

TABLE 3. Experimental conditions for data in figures 4–7.

Our G^*_{BT} values at different pressure levels are replotted in figure 10 along with values from the literature for gases. The data of Regnier & Kaplan (1963) were determined in flow adjacent to a vertical isothermal plate in pressurized carbon dioxide. The vertical ordinate in their study, with an isothermal surface condition, is in terms of G instead of G^*, where $G = 4(\frac{1}{4}Gr_x)^{\frac{1}{4}}$. Two dashed lines of the same slope as that which fits the present data collect their data points at $x = 12{\cdot}5$ and 25 cm fairly well, except for one point at $x = 25$ cm and $P = 1$ atm. This could be due to very low resolution of the interferometer output for such a low value of ΔT, 2 °C at this condition.

Clearly, G^* alone does not correlate the beginning of transition. Additional dependence on x and P, or equivalently on q'' and ν, arises in the manner shown. The significance of these results is discussed later in § 4.

3.2. *Mean and disturbance fields*

Mean and disturbance quantities in both velocity and temperature fields were measured for the range of parameters shown in figure 3. Typical test conditions are given in table 3 and are those used in figures 4–7. The detailed mean and disturbance field distributions are given in figures 4–10 of Mahajan (1977). Only the mean quantities are presented here to bring out the salient features of interest.

Mean velocity data. Measured velocity-component distributions are plotted in figure 4 in terms of normalized quantities $U/U_{\max}$ and $\eta = y/\delta$, where $\delta = 5x/G^*$ is the calculated laminar boundary-layer thickness, y is the physical distance normal to the surface and U and $U_{\max}$ are the local value and measured maximum value of the tangential velocity. For $x = 22$ cm and $G^* = 434$ at $P = 8{\cdot}36$ atm, we see that the measured velocity profile is in good agreement with the calculated laminar profile. The measured $U_{\max}$ value also matched the calculated $U_{\max L}$, where L refers to the laminar

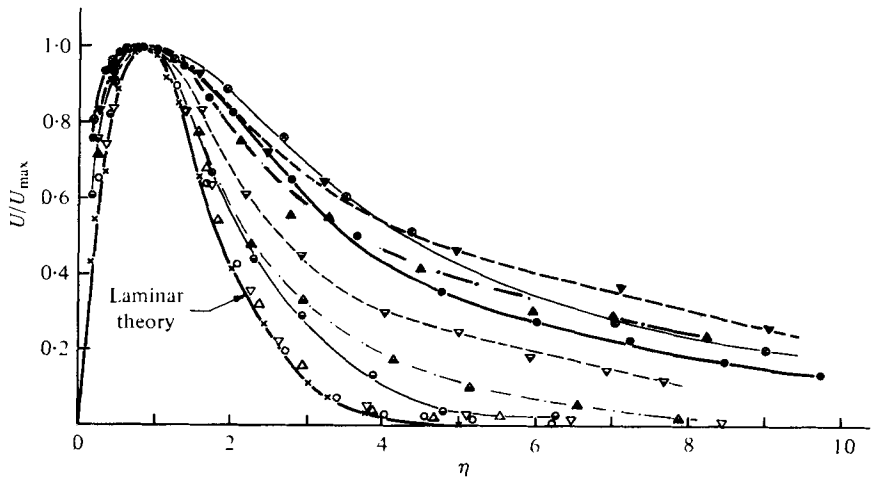

FIGURE 4. Comparison of transitional mean velocity distributions at different downstream locations and pressures. For notation, see table 3.

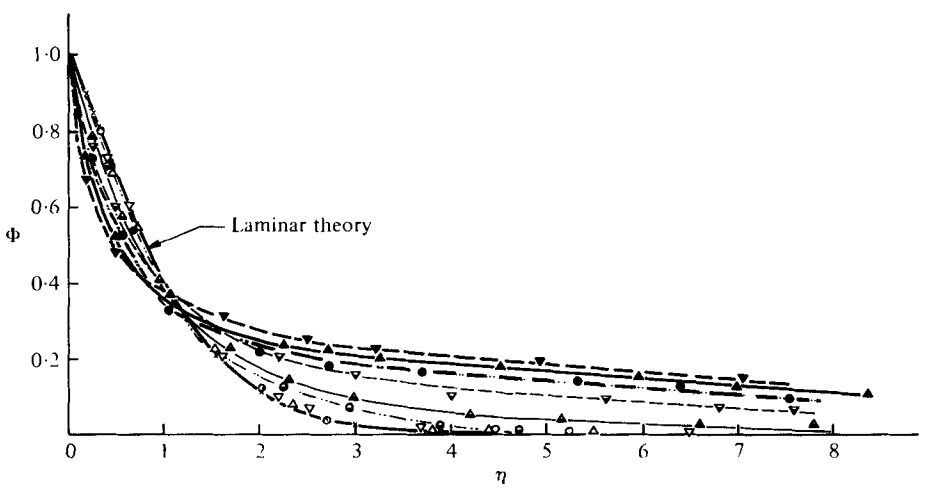

FIGURE 5. Comparison of mean temperature profiles for different downstream locations and pressures. For notation, see table 3.

flow; see figure 6. However, at $G^* = 470$, U_{max} was already about 4 % below the laminar value, indicating that transition had already begun. The accuracy and consistency levels of these measurements is very high, recall figure 1. The mean profile has also begun to deviate (figure 4). Further downstream, as a result of increasing turbulence, the deviations in form increase. The flow region thickens. The profile in the outer region is progressively flattened, although this trend ceases at $G^* = 611$.

Another important point that emerges from the profiles in figure 4 is the dependenc of their form on both x and P in addition to G^*. Consider first the results at $P = 8{\cdot}36$ atm for different downstream locations. At $x = 33$ cm and $G^* = 560$, the distribution has just deviated from laminar. However, at $x = 22$ cm it has already changed considerably at $G^* = 503$. Likewise, at $G^* = 611$, as we shall see later, transition is already complete at $x = 22$ cm. However, for $x = 33$ cm, it is still in progress at $G^* = 650$. Consider also

the data at $P = 4{\cdot}18$ and $8{\cdot}36$ atm. at the same value of $x = 33$ cm. Again, the dependence of mean velocity distributions on both pressure and G^* is evident. At the lower pressure, transition has already begun at $G^* = 514$. At the higher pressure, it does not begin until $G^* = 560$. Similarly at $G^* = 660$ at $P = 4{\cdot}18$ atm, transition appears to be complete, while at $P = 8{\cdot}36$ atm at $G^* = 650$, it is still in progress. These results confirm that any correlation of both ends of the transition process for gases must include a dependence on both x and P, in addition to G^*.

Mean temperature profiles. Measured mean temperature profiles for the same conditions as in figure 4, in terms of $\phi = (t-t_\infty)/(t_0-t_\infty)$, are plotted *vs.* η in figure 5. Here t, t_0 and t_∞ are the local fluid, surface and ambient fluid temperatures, respectively. Surface temperatures were obtained by extrapolating the measured temperature distributions to the foil surface. More closely spaced measurements were taken near the wall for more accurate extrapolation.

For $x = 22$ cm and $P = 8{\cdot}36$ atm, the temperature profile at $G^* = 470$ is in good agreement with the laminar profile. The experimental value of $\Delta T = t_0 - t_\infty$ was found to agree with the calculated laminar value of ΔT. Note that at this value of G^*, velocity transition had already begun. This indicates delayed thermal transition. However, at $G^* = 503$, the measured ΔT has already begun to deviate from the laminar one (see figure 6), indicating the beginning of thermal transition. Further downstream, the profiles progressively change from that for laminar flow. The thermal boundary layer thickens. The profiles steepen at low η and flatten at higher η. These deviations follow those of velocity field, as expected, since they are initially completely coupled. As the flow penetrates further into the ambient fluid, it diffuses the warm fluid outwards, thereby thickening the thermal layer. This modification is almost complete by $G^* = 611$. Further variation with increasing G^* is small. The independent effects of x and P, in addition to G^*, are seen in figure 5 as well as in figure 4.

The disturbance field distributions (see Mahajan 1977) lead us to conclude that, as for mean quantities, disturbance data during transition are also not correlated by G^* alone. The independent effects of x and P must also be considered.

3.3. *Variation of disturbance amplitude level downstream*

Changing disturbance and mean flow conditions downstream during transition are plotted in figure 6 in terms of G^*. The disturbance quantities are t' and u', the maximum measured amplitudes of the temperature and velocity disturbances, respectively. They are normalized by measured local mean flow values, the first by $t_0 - t_\infty$ and the second by $U_{\max}$. Disturbance quantities are shown in the bottom part of the figure. For the same conditions, the measured mean flow quantities, $U_{\max}$ and $t_0 - t_\infty = \Delta T$, normalized by local calculated laminar values at the same conditions, are plotted in the upper half of the figure. Velocity data are shown for all the conditions in table 3. However, since the temperature data exhibit very similar characteristics, we have plotted it only for $x = 22$ cm and $P = 8{\cdot}36$ atm, for various values of q''.

First, we note that the beginning of velocity transition, detected as a sudden decrease in $U_{\max}/(U_{\max})_L$ as discussed above, is also accompanied by a rapid increase in the magnitude of u'. Similar correspondence is seen in the temperature data. With further increases in G^*, disturbance magnitudes increase. They reach a maximum and then perhaps decrease. We shall see later that this distinct trend is associated with the end of transition. Similar behaviour at the end of transition was noted by Cheesewright (1968)

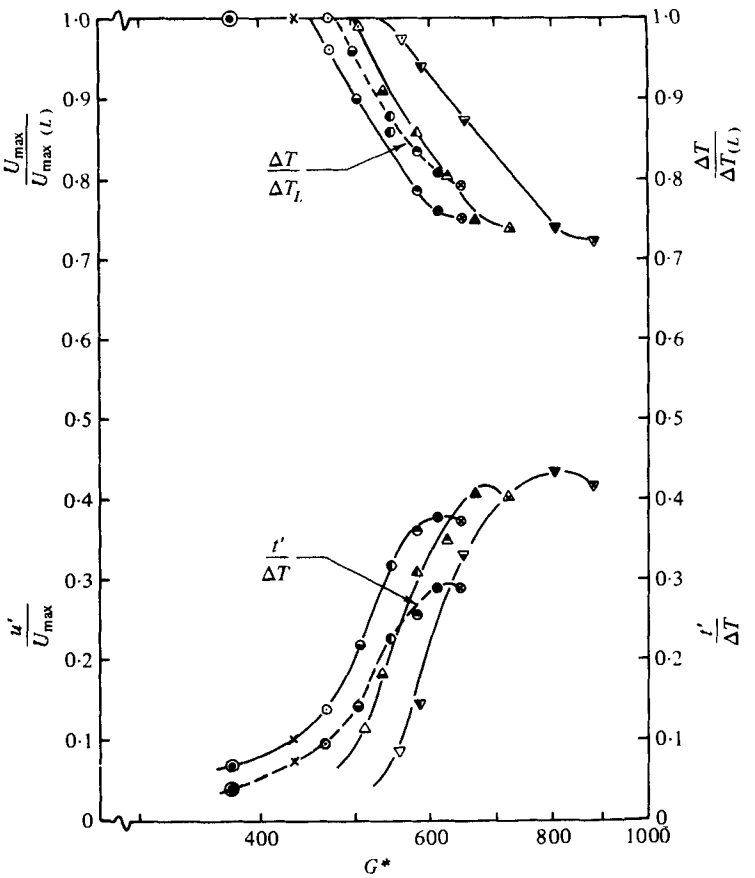

FIGURE 6. Downstream variation of disturbance level, excess temperature and maximum mean velocity. ——, velocity data; – – –, temperature data. For notation see table 3.

in air and by Jaluria & Gebhart (1974) and Bill & Gebhart (1978) in water. Coupled with these trends is the behaviour of the mean flow quantities $U_{max}/U_{max\,L}$ and $\Delta T/\Delta T_L$. Both decrease with increasing G^*, the rate of decrease becoming smaller as the end of transition is approached. After the completion of transition, they both appear to approach constant values.

The measured velocity and temperature disturbance amplitudes at the end of transition are seen to be of the order of 40 and 30 %, respectively. In water, Jaluria & Gebhart (1974) found the comparable values to be 50 and 70 % respectively. In early turbulence, Bill & Gebhart (1978) found the turbulent intensity $\overline{(u'^2)}^{\frac{1}{2}}/U_{max}$ to be about 24 %. In comparable forced flows, the level of turbulence intensity is relatively lower. For example, Klebanoff (1954) reported a value of 12 %. These results lead us to conclude with Lock & Trotter (1968), Godaux & Gebhart (1974) and Jaluria & Gebhart (1974) that the scale or intensity of turbulence in natural convection flows is relatively very high.

3.4. *Development of turbulence*

This aspect is often considered in terms of the development of local intermittency factors I_V or I_T. They are defined as the fraction of the total time during which the

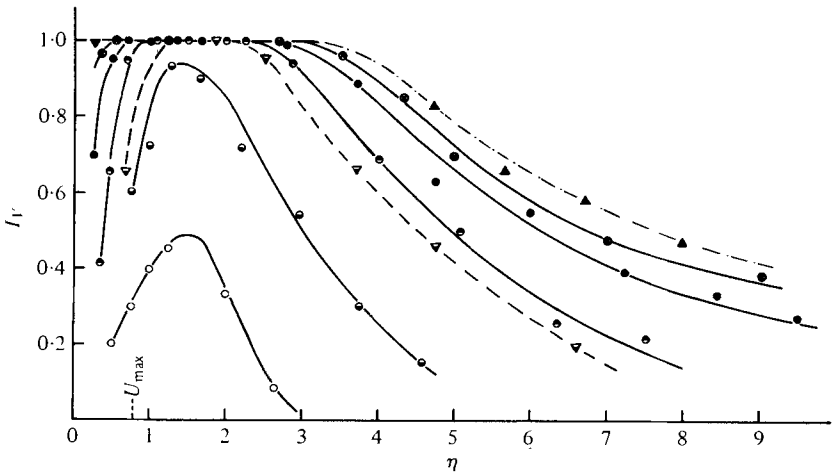

FIGURE 7. Velocity intermittency distributions across the boundary layer. For notation, see table 3.

flow at any point is turbulent, in the velocity and temperature fields, respectively. The presence of turbulence was judged as the superposition of aperiodic disturbances on the base flow. Characteristic I_V distributions so obtained across the boundary region are plotted in figure 7. The corresponding distributions of I_T are almost identical and are not shown.

For $x = 22$ cm, $P = 8{\cdot}36$ atm and $G^* = 470$, I_V increases with distance from the wall, and reaches a maximum very close to the inflexion point, at $\eta = 1{\cdot}50$. It then drops sharply to zero. With increasing G^*, the position of the peak is shifted towards the location of $U_{\max L}$, indicating better mixing in this region than in the outer one. The intermittency rapidly increases and spreads in both directions from the inflexion point. At $G^* = 611$, $I_V = 1$ over the boundary region from $\eta = 0{\cdot}70$ to $2{\cdot}75$, indicating full turbulence. Turbulence progressively reaches much further out. Even at $\eta = 9$, the flow is turbulent 30 % of the time. All the curves drop sharply towards the surface, indicating damping. After a certain level of G^*, the form of the distribution changes little.

Also shown are I_V distributions for several other experimental conditions. For example, at $G^* = 650$ for $x = 33$ cm and $P = 8{\cdot}36$ atm, the I_V curve is still in its evolving form and the intermittency level is lower than that for $G^* = 648$ at $x = 22$ cm. Likewise, comparison of the curves at $x = 33$ cm for $P = 4{\cdot}18$ and $8{\cdot}36$ atm, at about the same value of $G^* = 650$, shows that the distributions are different. Again G^* is not the indicator.

3.5. *Predominant frequencies of natural disturbances*

The frequencies of the amplified naturally occurring disturbances were determined from our disturbance amplitude data. They were converted to B^*; see § 3.1. We have already indicated that the data points in the upstream laminar flow agree extremely well with the predictions of linear stability theory. Further downstream, during transition, we found that a single disturbance frequency still dominated the remaining laminar portion of the flow. It was found to be constant across the boundary region. These data points are indicated by partially or fully shaded symbols on the stability

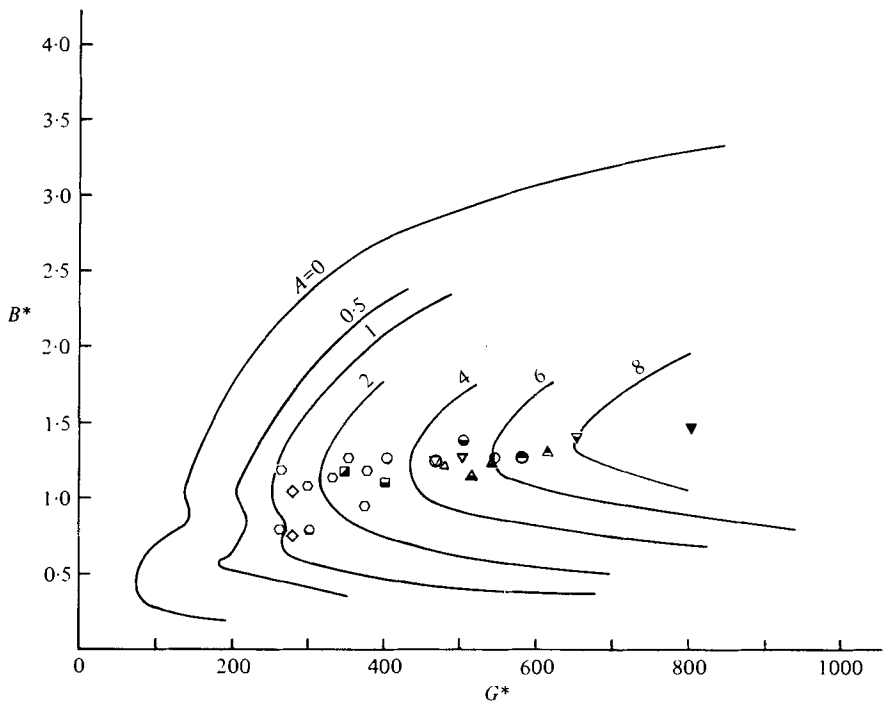

FIGURE 8. Stability plane for $Pr = 0{\cdot}733$ showing the measured disturbance frequency in the unstable laminar flow (open symbols) and in locally laminar portions of the flow in the transition region (partially or fully shaded symbols).

	x (cm)	P (atm)		x (cm)	P (atm)		x (cm)	P (atm)
⬡	13·2	15·92	○	22	8·36	△	33	4·18
□	13·2	8·36	▽	33	8·36	◇	33	2·05

plane in figure 8. All lie very close to the path of maximum disturbance amplification. Thus the highly selective amplification predicted by linear stability theory extends well beyond the range of linear processes, as first pointed out by Gebhart (1969), even for gases at high pressure. This agreement of theoretical predictions with experimental data, over a wide range of Prandtl numbers, has been summarized by Gebhart & Mahajan (1975).

The turbulent portion of the record showed higher frequencies. However, we were not able to determine a single dominant value, as found in water by Jaluria & Gebhart (1974). Our records were not primarily sinusoidal. A spectrum analysis would be necessary in a further investigation of this apparent difference in behaviour.

3.6. *Structure of turbulence across the boundary layer*

A sample of the actual analog records is reproduced in figure 9. These were taken at four different locations across the boundary layer at $G^* = 611$. Both velocity and temperature fluctuations are shown. The short lines shown on the left of the figure represent the mean values of temperature and velocity outputs. In the trace at $\eta = 0{\cdot}35$, close to the wall, the disturbance peaks occur almost equally in both directions relative to the mean. They also have a relatively lower amplitude,

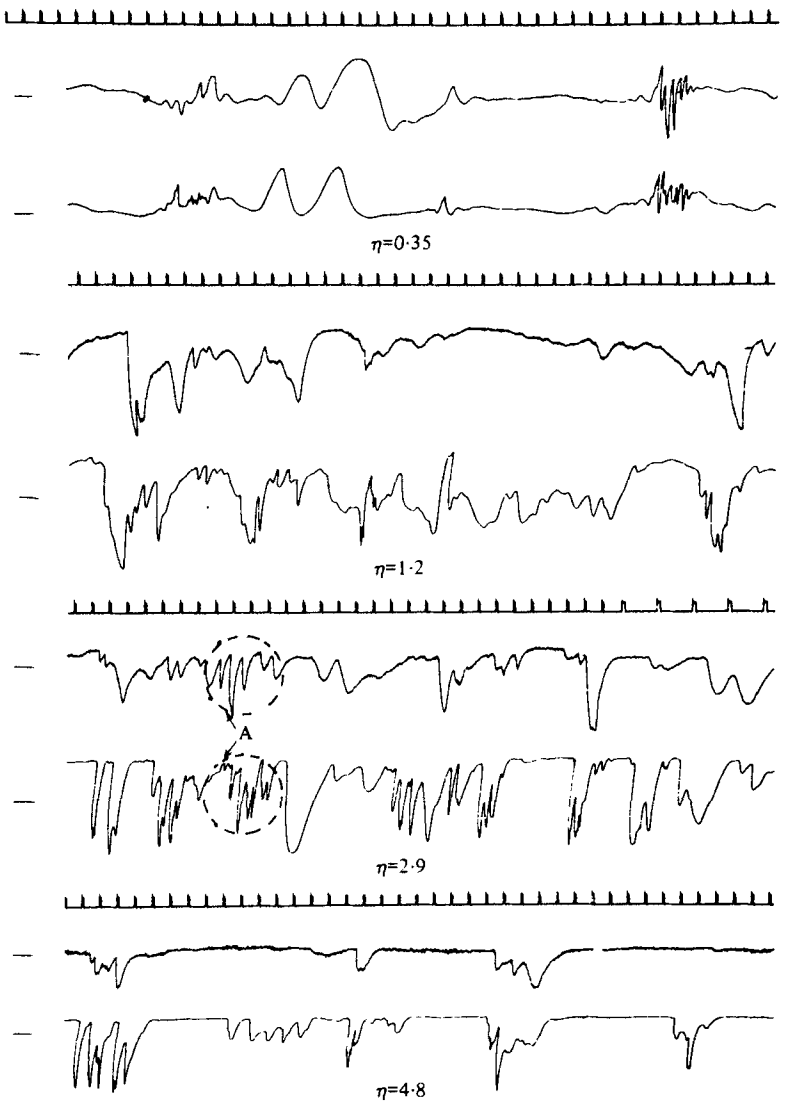

FIGURE 9. Temperature (upper trace) and velocity (lower trace) fluctuations across the boundary layer at $G^* = 611, P = 8{\cdot}36$ atm. $x = 22$ cm. Scale: temperature, 20 μV/cm; velocity, 100 mV/cm.

indicating damping. Further out, towards the middle of the boundary layer at $\eta = 1{\cdot}2$, they are still in both directions, but larger in amplitude. However, in the outer portion, at $\eta = 2{\cdot}9$ and $4{\cdot}8$, the sharp disturbance deflexions are largely on the positive side, indicating asymmetry. These are typical of all of our records. Similar results were reported by Lock & Trotter (1968) for their measurements in water.

These records also illustrate the expected direct coupling between velocity and thermal disturbances. The temperature follows the slow frequency fluctuations in velocity, but not the most rapid oscillations; see the portion marked *A* in the figure. This follows from the passive nature of the thermal field.

3.7. *End of transition*

This condition was taken as the downstream location beyond which the intermittency distributions I_V and I_T showed no appreciable further change in form. This is the criterion used by Jaluria & Gebhart (1974). Our results also show that the temperature and velocity transitions end simultaneously.

Considering again figure 7, for $x = 22\,\text{cm}$ and $P = 8{\cdot}36\,\text{atm}$, the intermittency distributions are seen to change progressively as G^* increases from 470 to 611. However, the further change as G^* increases to 648 is small, signalling the end of transition at about $G^* = 611$. Figure 6 indicates that the variations of both $U_{\max}/U_{\max L}$ and $\Delta T/\Delta T_L$ show a sharply changing trend at about $G^* = 611$. They quickly attain an almost constant value. Also, the relative velocity and temperature disturbance amplitudes reach a maximum around $G^* = 611$ and then decrease further downstream. All measures clearly signal changes in flow regime.

Our measured values of G^*_{ET}, where ET means end of transition, are also plotted in figure 3, as the solid points. At each pressure level the x, q'' interdependence was

$$G^*_{ET} \propto x^m, \tag{3}$$

where $m \simeq 0{\cdot}5$. At a given location x, at different values of q'' we find the pressure dependence to be

$$G^*_{ET} \propto P^n, \tag{4}$$

where $n \simeq \frac{1}{3}$. This variation is also shown in figure 11, where our G^*_{ET} data are plotted *vs.* P, along with the other data pertaining to the completion of transition in gases. Thus the end of transition is additionally dependent on x and there is also a very strong P or ν effect.

4. Correlation of the extent of the transition regime

Relations (1)–(4) indicate how the beginning and end of transition depend upon x and P. The region close to these boundaries was mapped using small step changes in heat flux. These measurements of x and P allowed the above G^*_{BT} and G^*_{ET} dependences to be measured sharply. These relations are generalized below.

4.1. *Proposed parameter for the beginning of transition*

The transition conditions (1) and (2) are incorporated into the following single relation:

$$\frac{G^*_{BT}}{x^{\frac{2}{5}}}\,\rho^{-\frac{2}{15}} = \text{constant}. \tag{5}$$

This form is then non-dimensionalized into the parameter Q_{BT} for the beginning of transition as given below. Recall that $\nu \propto \rho^{-1}$ and the definition of G^*. Hence

$$\left(\frac{q''}{g\mu}\right)^{\frac{1}{5}} \left(\frac{gx^3}{\nu^2}\right)^{\frac{2}{15}} = qB^{\frac{2}{15}} = Q_{BT} = \text{constant}, \tag{6}$$

where $q = (q''/g\mu)^{\frac{1}{5}}$ is the fifth root of the non-dimensional local heat flux to the boundary-region flow and B is the unit Grashof number gx^3/ν^2. All properties are evaluated at the ambient temperature. Our data give the values of Q_{BT} for the beginning of velocity and thermal transition in nitrogen as 290 and 305, respectively.

There are several other ways to modify the relation in (5). For example, it may also be rewritten as

$$G^*_{BT}\left(\frac{\nu^2}{gx^3}\right)^{\frac{1}{15}}\left(\frac{g\beta_t x}{c_p}\right)^{-\frac{1}{5}} = \text{constant}, \tag{7}$$

where c_p is the specific heat at constant pressure. The last quantity in (7) arises as a measure of the importance of the viscous dissipation and pressure terms in the energy equation; see Gebhart (1971, p. 324). It is very small in gases unless g and/or x are very large or T is small, and in liquids if g, x and/or Pr are large; see Gebhart (1962). For the conditions of our experiments and all other experiments reported here, it is negligible compared with other terms retained in the energy equation. It is, therefore, not a promising parameter with which to characterize transition. Other methods of non-dimensionalizing in (5) encounter similar questions of relevancy. On the other hand, the parameter in (6) is relatively simple in form. It also may be simply interpreted as a flux q and a unit Grashof number gx^3/ν^2.

We now compare Q_{BT}, with the kinetic energy flux parameter $E = G^*B^{-\frac{2}{15}}$, which was proposed by Jaluria & Gebhart (1974) as a correlator of the beginning of transition on the basis their data in water. As noted in § 3.1, the G^*_{BT} dependence on x, implied by both Q_{BT} and E, is the same. However, the dependence $G^*_{BT} \propto \nu^{-\frac{2}{15}}$ which we found in pressurized nitrogen is different from the dependence $G^*_{BT} \propto \nu^{-\frac{4}{15}}$ used to non-dimensionalize E. This difference is not in fact an important one. The investigation by Jaluria & Gebhart (1974) in water at essentially constant temperature did not assess a ν effect. It was introduced on dimensional grounds. In our experiment, ν was changed by a factor of about 16. The other transition data in pressurized gases obtained by Regnier & Kaplan (1963) also support the present G^*_{BT} dependence on ν; see figure 11. However, the above difference in the exponent of ν in Q_{BT} and E does produce a substantial and large difference in their meaning. The parameters E and Q_{BT} differ by the following function of fluid properties:

$$Q_{BT} = G^*\left(\frac{\nu^2}{gx^3}\right)^{\frac{2}{15}}\left(\frac{k\nu^{-\frac{2}{3}}}{5^4 g^{\frac{2}{3}}\beta_t \mu}\right)^{\frac{1}{5}} = Ek_1, \tag{8}$$

where k_1 is a constant which depends upon the property group defined in (8). For water at $Pr = 6{\cdot}7$, $k_1 = 25{\cdot}07$.

Thus E may still be used to correlate the beginning of transition, where the kinematic viscosity of the ambient fluid has a given value, as it indeed is for the data of Jaluria & Gebhart (1974). It also correlates other data in water well over a small range of ν; see table 1 of their paper. However, for gases, Jaluria & Gebhart indicate values of E about 60 % higher than in water. The new parameter Q_{BT} is more general. We shall see that a single value of Q_{BT} defined reasonably well the beginning of transition, both in gases and liquids.

4.2. *Comparison with the other data in gases*

Our data and those of others concerning the beginning of transition in gases are summarized in table 1 and are also plotted in figure 10. The local flow conditions are tabulated. The downstream locations, where not stated in other studies, have been estimated as accurately as the descriptions of the experiments permitted. Some uncertainty arises here, as discussed in detail by Qureshi & Gebhart (1978).

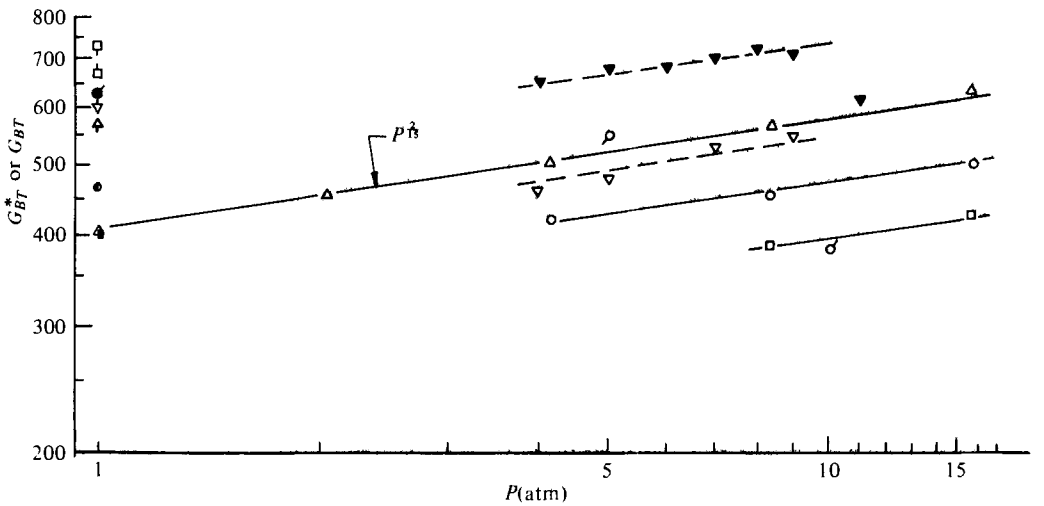

FIGURE 10. Beginning of transition data in gases. Present data: □; x = 13·2 cm; ○, x = 22 cm; △, x = 33 cm. For other data, see table 1.

Recall that, for an isothermal surface, the local heat flux q'' in laminar flow is given as

$$q'' = k\Delta T \frac{G}{4x}[-T'(0)], \tag{9}$$

where $[-T'(0)]$ is a Prandtl number dependent constant which is given, for example, in table 8.1 of Gebhart (1971). The laminar relation is justified at the beginning of transition and was used to compute the values of q'' in the determination of Q_{BT} for isothermal surfaces.

The tremendous scatter in the G^*_{BT} or G_{BT} values in table 1, both at 1 atm and at higher pressure levels, represents the failure of the Grashof number to predict the beginning of transition. However, when converted to Q_{BT}, all data wherein a local sensor, either a hot-wire or thermocouple probe, was used to detect the beginning of transition move close to our values of 290 and 305, for the beginning of velocity and thermal transition, respectively, the maximum difference being of the order of 15 %; see the last column. Considering that the criteria used for the beginning of transition in these studies do not correspond to exactly equivalent stages of transition, we consider this agreement to be good. The interferometer determination results in a number of substantially higher values of Q_{BT}. This discrepancy is thought to be due to the insensitivity of the interferometer to small and/or concentrated turbulence. This is analogous to the differences noted in data for transition in supersonic boundary layers between schlieren measurements and thermocouple measurements, as noted by Schubauer & Klebanoff (1956). Bill & Gebhart (1975) reached the same conclusion, concerning interferometry, from their study of transition in plane plumes. The lower values of Q_{BT} for two data points of Regnier & Kaplan (1963) could also be due in part to inaccurate resolution of interferometer output for low values of ΔT for these points. Earlier transition is suggested by the lower value of Q_{BT} for the data of Eckert & Soehngen (1951). This is possibly due to the particular nature of their experiment. Very high disturbance levels were present and the flow was actually a transient cooling of a surface.

The fact that our parameter based on a uniform-flux surface condition correlates

well the data for an isothermal surface condition is not surprising. It was noted by Hieber & Gebhart (1971) and by Jaluria & Gebhart (1974) that the two cases are directly related to each other in terms of G and G^*. This equivalence was taken as the basis for the determination of q'' in the calculation of Q_{BT} for isothermal surfaces. There may also be concern that the stability characteristics for the two different bounding conditions for temperature disturbances could be quite different. Then there would be little reason to expect universality of the new transition parameter. However, differences in the amplification-rate contours, for the two extreme boundary conditions on temperature oscillations, have been shown to be significant only at low values of the Grashof number. In the range of Grashof numbers at which transition occurs, the difference in the contours is small indeed; see, for example, figures 1 and 2 of Hieber & Gebhart (1971). Therefore the new parameter should be expected to correlate the beginning of transition for differing surface conditions, as indeed it does.

4.3. *Prandtl number effect*

The relative thickness of the velocity and thermal boundary regions in laminar flow depends on the Prandtl number. This has been shown to have a large effect on instability and on disturbance growth rates. We have assessed any residual dependence of Q_{BT} on Pr. Transition data in water (Pr = 5–11) are collected in table 2, along with calculated values of Q_{BT}. As in gases, these results were obtained with different heating conditions, methods of observation and criteria for transition. A direct comparison is, therefore, not possible for all of the data. However, the study of Jaluria & Gebhart (1974), in water at $Pr = 6{\cdot}7$, is very similar to the present work in both experimental and instrumental methodology. They are compared to assess any residual Prandtl number effect. In both of these studies the velocity transition occurs first. Since it is the first important step in a long process of breakdown of transition, velocity transition data are used to evaluate the Prandtl number effect.

The value of $E = 13{\cdot}6$ found by Jaluria & Gebhart (1974) becomes $Q_{BT} = 341$ compared with 290 in this study. The difference is about 17 %. We shall see later that this is partially due to the effect of property variation across the boundary layer.

Note that the parameter Q_{BT} is independent of k. Although our experiments were not designed to test this specifically, the small difference in the values of Q_{BT} for gases ($k \sim 0{\cdot}00026$ W/cm °C) and for water ($k \sim 0{\cdot}006$ W/cm °C) indicates that the incorporated k independence in Q_{BT} is entirely appropriate.

4.4. *End of transition*

A parameter given below correlates our data for the end of transition. It is non-dimensionalized in terms of B and Q as follows:

$$\frac{G^*}{x^{0{\cdot}5}}\rho^{-\frac{1}{5}} \propto (Q'(x)\frac{\beta_t}{k}\,Pr\,5^4)^{\frac{1}{5}}\left(\frac{gx^3}{\nu^2}\right)^{\frac{1}{3{\cdot}6}} = QB^{\frac{1}{3{\cdot}6}} = Q_{ET}, \tag{10}$$

where $Q' = q''x$ and therefore Q is the fifth root of the non-dimensional total heat convected by the boundary layer at x. The value from our experiment is $Q_{ET} = 11{\cdot}4$. This parameter may also be recast as

$$Q_{ET} = G^*(\nu^2/gx^3)^{\frac{1}{5}}\,Pr^{\frac{1}{5}} = 5^{\frac{1}{5}}Ra^{*\frac{1}{5}}B^{\frac{1}{5}},$$

where $Ra^* = Gr_x^*\,Pr$ is the Rayleigh number for the uniform-flux surface condition.

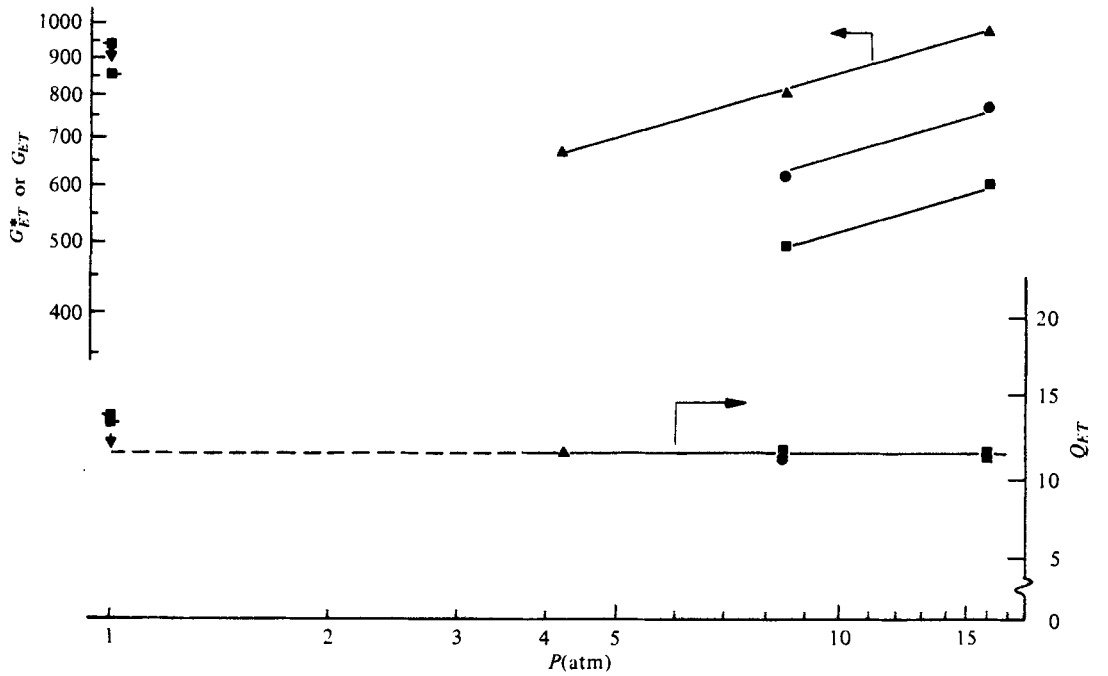

FIGURE 11. End of transition data in gases. Present data: ■, x = 13·2 cm; ●, x = 22 cm; ▲, x = 33 cm. For other data, see table 1.

Our data and other data pertaining to the completion of transition in gases are summarized in table 1 and the values of G^*_{ET} or G_{ET} are plotted in figure 11. As for the beginning of transition (figure 10), there is much scatter. However, the observation made with a local sensor by Cheesewright (1968), when converted to the form of Q_{ET}, becomes close to our value of Q_{ET} = 11·4. The comparison, in terms of Q_{ET}, is also shown in figure 11. As for the beginning of transition, the interferometric results of Hugot, Jannot & Pirovano (1971) result in a higher value of Q_{ET}. Note that the data of Cheesewright and of Hugot *et al.* are for an isothermal surface condition. They were converted to Q_{ET} using (8), with $-T'(0)$ taken as the value estimated from the data at the end of transition. The laminar value of $-T'(0)$, used at the beginning of transition, may not be used later during transition, where it may differ from the measured value by as much as 60 %.

We select again the data of Jaluria & Gebhart (1974) to assess the performance of Q_{ET} as a correlator of the end of transition in water (Pr = 6·7). The average value of Q_{ET} from their data is 11·0; see table 2. This is only about 4 % lower than our value.

4.5. *Predictive parameters for transition limits*

We have seen that unique values of our transition parameters Q_{BT} and Q_{ET} correlate beginning and end of transition. The value for the beginning of velocity transition in both gases and water is Q_{BT} = 290. Thermal transition follows at 305 in gases and at 384 in water (Pr = 6·7). The latter value is obtained by converting E = 15·2, given by Jaluria & Gebhart (1974), to Q_{BT}. Velocity and thermal transition end simultaneously at $Q_{ET} = QB^{\frac{1}{10}}$ = 11·4.

These predictions are also compared in table 2 with the other data for water ($Pr = 5{\cdot}05$–11). We compared the data at different Prandtl numbers but at about the same value of ΔT across the boundary region. The values of both Q_{BT} and Q_{ET} are close, thus lending support to the generality of these correlations. However, the data for higher values of ΔT indicate higher values of both Q_{BT} and Q_{ET}; see, for example, those of Vliet & Liu (1969), where very substantial property variations are present. To assess this, values of $\epsilon = \mu_\infty/\mu_0$ are listed in table, where μ_0 and μ_∞ are, respectively, the values of the absolute viscosity at the wall and ambient temperatures. Clearly, the effect of a larger ϵ (or ΔT) is to delay the beginning of transition in water, in terms of Q_{BT}. In gases, on the other hand, the effect of ΔT seems to be destabilizing but weak. In our experimental range of $\Delta T \simeq 2$–$80\,^\circ\mathrm{C}$, the value of Q_{BT} at $\Delta T \simeq 80\,^\circ\mathrm{C}$ was only 4 % lower than at $\Delta T \simeq 2\,^\circ\mathrm{C}$.

Thus a viscosity increase outwards across the boundary region appears to stabilize the flow in both water and gases. These effects of property variation on the beginning of transition in gases and water are similar to those predicted in forced flow by the perturbation analysis of Hauptmann (1968). The effect may be partially responsible for the higher values of Q_{BT} from the data of Jaluria & Gebhart (1974), for water, compared with ours for nitrogen.

Considering the end of transition Q_{ET}, the data in table 2 again indicate a similar dependence on property variations. However, since these experiments were not designed to determine such effects, we have not attempted here a quantitative evaluation of their influence.

5. Conclusions

Experimental measurements of both velocity and temperature transition have been made in pressurized nitrogen. Both mean flow and disturbance data were determined at different downstream locations and pressures. The laminar results are in good agreement with existing boundary-layer and stability theories.

The mean temperature data during transition are in reasonable agreement with the few past experimental studies at 1 atm. However, these are the first data in gases for the mean velocity field adjustment during transition. Our results map the process of transition in terms of the development of both the mean and the disturbance profiles for both the velocity and the temperature field.

The largest amplitude disturbances first appear near the inflexion point in the laminar velocity profile. They are very quickly reflected in the thermal boundary layer, since the layers overlap. They are impressed on the inner region and eventually initiate velocity and thermal transition almost simultaneously. The deviation of mean profiles is accompanied by an increase in boundary-layer thickness, and by increasing disturbance frequency and rate of disturbance growth. As the end of transition is approached, there is a decreasing rate of change of both mean and disturbance quantities. Finally, the end of transition is simultaneously marked by no appreciable further change in the intermittency distribution, by the beginning of a decrease in disturbance amplitude and by little further change in both $U_{\max}/U_{\max L}$ and $\Delta T/\Delta T_L$.

Velocity and thermal disturbances are closely coupled. Temperature disturbances follow low frequency velocity fluctuations more closely, owing to the passive nature of the temperature field. Local sensor measurements reveal that these disturbances are

asymmetric in the outer part of the boundary region and essentially symmetric elsewhere. In the inner region, the surface damps disturbance intensity.

The disturbance frequency data lend strong support to the linear stability theory. The measured values of the frequency enabled detailed verification of the relatively unexplored portion of the calculated stability plane immediately following initial instability. This is the first experimental verification in gases of the predicted buoyancy coupling in disturbance growth. Further downstream, the frequencies are again found to lie on the path of most amplified frequencies. During transition a single characteristic frequency was observed in the locally laminar flow, in continuing agreement with the prediction of linear theory of frequency filtering. In the turbulent portion, a spectrum of frequencies arose.

None of the events of transition are correlated by G^* alone. The additional dependence on x and ν is very strong. The beginning of transition appears to occur when a parameter of the form $Q_{BT} = qB^{\frac{2}{15}}$ has reached a certain value. Here q is the fifth root of the non-dimensional heat flux and B is the unit Grashof number. The end of transition, on the other hand, has been correlated by the parameter $Q_{ET} = QB^{\frac{1}{15}}$, where Q is the fifth root of the non-dimensional total heat convected locally by the boundary layer. A re-examination of the other studies of transition, both in gases and in liquids, supports both correlations. In addition, the total body of existing transition data shows a regular dependence of the predictive parameters on property variation across the boundary region. Further analytical and experimental work is necessary to assess such effects.

The authors wish to express their appreciation for the support of the National Science Foundation under Grant ENG 7522623 and of Prof. D. L. Turcotte for useful discussions on the formulation of the transition parameters.

REFERENCES

AUDUNSON, T. & GEBHART, B. 1976 Secondary mean motions arising in a buoyancy induced flow. *Int. J. Heat Mass Transfer* **19**, 337–350.

BILL, R. G. & GEBHART, B. 1975 The transition of plane plumes. *Int. J. Heat Mass Transfer* **18**, 513.

BILL, R. G. & GEBHART, B. 1978 Development of turbulent transport in vertical natural convection boundary layer. To be published.

CHEESEWRIGHT, R. 1968 Turbulent natural convection from a vertical plane surface. *J. Heat Transfer* **90**, 1–8.

COLAK-ANTIC, P. 1964 Hitzdraht messungen des laminar-turbulenten Umschlagas bei freier Konvektion. *Jahrbuch der WGLR* pp. 1972–1976.

DRING, R. P. & GEBHART, B. 1968 A theoretical investigation of disturbance amplification in external laminar natural convection. *J. Fluid Mech.* **34**, 551–564.

ECKERT, E. R. G., HARTNETT, J. P. & IRVINE, T. F. 1960 Flow visualization studies of transition in turbulence in free convection. *A.S.M.E. Paper* no. 60-WA-250.

ECKERT, E. R. G. & SOEHNGEN, E. 1951 Interferometric studies on the stability and transition to turbulence of a free-convection boundary layer. *Proc. Gen. Disc. Heat Transfer, London*, pp. 321–323.

GEBHART, B. 1962 Effects of viscous dissipation in natural convection. *J. Fluid Mech.* **14**, 225.

GEBHART, B. 1969 Natural convection flow, instability and transition. *J. Heat Transfer* **91**, 293-309.

GEBHART, B. 1971 *Heat Transfer*, 2nd edn. McGraw-Hill.

GEBHART, B. 1973 Instability transition and turbulence in buoyancy-induced flows. *Ann. Rev. Fluid Mech.* **5**, 213–246.

GEBHART, B. & MAHAJAN, R. L. 1975 Characteristic disturbance frequency in vertical natural convection flow. *Int. J. Heat Mass Transfer* **18**, 1143–1148.

GODAUX, R. & GEBHART, B. 1974 An experimental study of the transition of natural convection flow adjacent to a vertical surface. *Int. J. Heat Mass Transfer* **17**, 93–107.

HAUPTMANN, E. G. 1968 The influence of temperature dependent viscosity on laminar boundary layer stability. *Int. J. Heat Mass Transfer* **11**, 1049–1052.

HIEBER, C. A. & GEBHART, B. 1971 Stability of vertical natural convection boundary layers: some numerical solutions. *J. Fluid Mech.* **48**, 625–646.

HUGOT, G., JANNOT, M. & PIROVANO, A. 1971 *Compte-redu de Fin de Contrat DGST* no. 69-01-773.

JALURIA, Y. & GEBHART, B. 1973 An experimental study of nonlinear disturbance behaviour in natural convection. *J. Fluid Mech.* **61**, 337.

JALURIA, Y. & GEBHART, B. 1974 On transition mechanisms in vertical natural convection flow. *J. Fluid Mech.* **66**, 309–337.

KLEBANOFF, P. S. 1954 Characteristics of turbulence in a boundary layer with zero pressure gradient. *N.A.C.A. Tech. Note* no. 3178.

LOCK, G. S. H. & TROTTER, F. J. de B. 1968 Observations on the structure of a turbulent free convection boundary layer. *Int. J. Heat Mass Transfer* **11**, 1225–1232.

MAHAJAN, R. L. 1977 Higher order effects, stability and transition in vertical natural convection flows. Ph.D. thesis, Cornell University.

MAHAJAN, R. L. & GEBHART, B. 1978 Hot-wire anemometer calibration for measurements in free, mixed and forced convection in pressurized nitrogen. *J. Heat Transfer*. To be published.

QURESHI, Z. & GEBHART, B. 1978 Transition and transport in a buoyancy driven flow in water adjacent to a vertical uniform flux surface. *Int. J. Heat Mass Transfer*. To be published.

REGNIER, G. M. & KAPLAN, C. 1963 Visualization of natural convection on a plane wall and in a vertical gap by differential interferometry. Transitional and turbulent regimes. *Proc.* 1963 *Heat Transfer Fluid Mech. Inst.* pp. 94–110. Stanford University Press.

SCHUBAUER, G. B. & KLEBANOFF, P. S. 1956 Contributions on the mechanics of boundary layer transition. *N.A.C.A. Rep.* no. 1289.

SZEWCZYK, A. A. 1962 Stability and transition of the free convection layer along a vertical flat plate. *Int. J. Heat Mass Transfer* **5**, 903–914.

VLIET, G. C. & LIU, C. K. 1969 An experimental study of turbulent natural convection boundary layers. *J. Heat Transfer* **91**, 517–531.

WARNER, C. 1966 Turbulent natural convection in air along a vertical flat plate. Ph.D. thesis, University of Michigan.

WARNER, C. & ARPACI, V. S. 1968 An experimental investigation of turbulent natural convection in air at low pressure along a vertical heated plate. *Int. J. Heat Mass Transfer* **11**, 397–406.